ELSEVIER

Journal of Nuclear Materials 307–311 (2002) 1624–1628

journal of nuclear materials

www.elsevier.com/locate/jnucmat

Micromechanical modeling of master curve temperature shifts due to constraint loss

G.R. Odette *, M.Y. He

Department of Mechanical and Environmental Engineering, University of California, Santa Barbara, CA 93106-5070, USA

Abstract

The effects of constitutive and local fracture properties on constraint loss effects in fracture toughness tests of small specimens was carried out within the framework of the MC-ΔT method. Constraint loss (CL) decreases the temperature at a specified reference toughness. This temperature shift increases with decreasing: (a) specimen size, (b) ratio of the critical cleavage stress to yield stress and (c) strain hardening. The toughness–temperature curve shift due to CL increases with higher reference toughness and reference toughness–temperature. These results can guide the development and interpretation of small specimen fracture tests, as well as the use of even smaller specimens for particular applications, like comparative studies of irradiation variable effects on embrittlement. While they are only briefly noted in this work, additional consideration of both statistical and three dimensional size effects will be carried out in the future.

1. Introduction – the MC-ΔT method

The design and operation of fusion first wall and blankets will require a quantitative prediction of the in-service fracture toughness–temperature curves, $K_{Jc}(T)$, of candidate bcc vanadium (e.g., V–4Cr–4Ti) and ferritic–martensitic steel alloys, as well as methods to use toughness data to predict the stress–strain limits of flawed structures that are embrittled by irradiation. Unfortunately, limited irradiation space generally dictates that irradiation effects on $K_{Jc}(T)$ must be evaluated with small to ultra-small specimens. Due to inherent statistical scatter in toughness data, direct measurements of $K_{Jc}(T)$ would require very large numbers of specimens. Further, combinations of many variables control irradiation embrittlement. Thus, even if very small specimens can be used, measuring a huge number of $K_{Jc}(T)$ curves for combinatorial combinations of key irradiation and material variables is clearly prohibitive.

Thus we have proposed a vastly more efficient and tractable alternative known as the master curves-(temperature) shifts (MC-ΔT) method [1]. The MC-ΔT method measures a *reference-temperature* (T_0) with a small number of relatively small specimens for limited family of fixed $K_{mc}(T - T_0)$ *shapes*. A particular reference T_{or} and reference $K_{mc}(T - T_{or})$ shape are applicable to a corresponding reference K_{Jcr} level and reference set of material, specimen geometry and test conditions. These are typically: $K_{Jcr} = 100$ MPa$\sqrt{\text{m}}$, unirradiated, deep cracks-small scale yielding, specimen thickness of 25 mm and static loading rates. The unirradiated T_{or} and shape may vary for a different set of conditions, such as shallow cracks or dynamic loading rates [1]. The pertinent reference MC shape and T_{or} is then shifted (ΔT_0) to account for additional effects irradiation, a different specimen size and/or geometry (resulting in constraint loss) and loading rate as $T_0 \approx T_{or} + \Delta T_{irr} + \Delta T_{cl} + \Delta T_{rate}$. One resulting advantage is that the various ΔT can be independently evaluated and modeled. For example, it is often possible to estimate ΔT_{irr} from tensile or even hardness data. Semi-empirical models can also be used

* Corresponding author. Tel.: +1-805 893 3525; fax: +1-805 893 8651.

E-mail address: odette@engineering.ucsb.edu (G.R. Odette).

0022-3115/02/$ - see front matter
PII: S0022-3115(02)01172-8

to relate the shifts to key irradiation (and material) variables like fluence (ϕt) and irradiation temperature (T_{irr}), $\Delta T_{irr} = f(\phi t, T_{irr}, \ldots)$. Another important advantage is that toughness evaluations can be tailored to thin-walled fusion structures, which differ appreciably from the normal application of heavy section fracture mechanics.

However, the use of small specimens and application to fusion structures must directly address the issue of '*size effects*' on toughness. Size effects may arise from both the weakest link statistics of the (highly) stressed crack tip volume and constraint loss (CL) due to deviations from small scale yielding conditions. The consequences of both mechanisms to the actual measured values of toughness, K_q, depend on the basic properties and microstructure of the alloy in question, as well as specimen size and geometry and loading level. Thus the objective of this work is to assess the effects of microstructurally mediated constitutive and local fracture properties on CL within the framework of the proposed MC-ΔT method. We also consider briefly statistical size scaling and loading rate effects.

2. The finite element based toughness scaling model

It has been shown elsewhere that a useful local measure of cleavage fracture toughness of a material is a critical crack tip stress contour ($\sigma_{22} \geqslant \sigma^*$) encompassing a critical area (A^*) or volume (V^*) of material [1]. The σ^*–A^* criterion is an extension of the classical Ritchie, Knott and Rice model based on a σ^* critical distance concept [2]. The σ^*–A^* model correctly predicts the shape of the MC at low temperatures (where σ^* is ≈constant) [3]. Further, the model can be used to adjust K_q data for size and geometry mediated CL [1]. Finally, the model provides a natural link between the σ^*–A^*–V^* micromechanics and weakest link statistical effects leading to a toughness scaling with crack front length (B) as $K_{Jc} \approx$ proportional to $B^{-1/4}$ ($V^* = BA^* \propto K_{Jc}^4$) [4].

The basic principle in adjusting for CL effects within this framework is to determine the K_q, for conditions deviating from small scale yielding, that produces the same A^* (or V^*) as the corresponding K_{Jc}, where $K_q > K_{Jc}$. Dodds and coworkers have formulated the CL adjustment in a particularly convenient non-dimensional form, recognizing that ratio of $K_q/K_{Jc} = (A_{ssy}/A_q)^{1/4}$ does not depend on the absolute value of A^*, but does depend on the materials constitutive law and σ^* [5,6]. Finite element (FE) methods can be used to determine the quantitative relation $K_q/K_{Jc} = f(K_q, \sigma_y/E, \sigma^*/\sigma_y, N)$ where E is the elastic modulus, σ_y is the yield stress and N represents the material post-yield strain hardening behavior (see below).

However rather than developing direct adjustments, we use the FE based $K_q/K_{Jc} = f(K_q, E/\sigma_y, \sigma^*/\sigma_y, N)$ relations to evaluate T_0 shifts within the framework of the MC-ΔT approach. This is done by specifying a reference T_{or} for a reference small scale yielding K_{Jcr} and then determining the lower T_{ocl} corresponding to the same toughness level in a specimen suffering CL. Physically, the same toughness can be achieved because σ_y increases with decreasing temperature $\sigma_y(T)$. Thus $\Delta T_{cl} = T_{or} - T_{ocl}$ depends on $\sigma_y(T)$, N (or other representations of strain hardening), $R = \sigma^*/\sigma_y$, b the uncracked ligament equal to the specimen width (W) minus crack length (a) (here for $a/W \approx 0.5$), T_{or} and K_{Jcr}. The T_{ocl} can be generally related to the loading index $M = Eb\sigma_y/K_{Jcr}^2$; note M depends only on b for specified values of K_{Jcr}, etc.

The 2D FE simulations were performed for the three-point bend specimen under the loading conditions from small to large scale yielding. The initial radius of the crack tip ρ is taken to be 0.001 W. The calculations are conducted using a general-purpose FE code, ABAQUS [7], with four node bilinear elements. The mesh was refined near the crack tip where the size of the smallest element is less than $\rho/10$. The benchmark results for the small scale yielding limit were determined by fits at low loading regime where the stressed area varies as J^2. A typical half specimen mesh has 4368 elements and 4519 nodes.

Two types of elastic–plastic constitutive equations were used:

$$\varepsilon/\varepsilon_y = \sigma/\sigma_y \quad \text{for } \varepsilon \leqslant \varepsilon_y, \tag{1}$$

$$\begin{aligned} &\sigma/\sigma_y = 1 \quad \text{for } \varepsilon_y \leqslant \varepsilon_y \leqslant \varepsilon_1, \\ &(\varepsilon - \varepsilon_1)/\varepsilon_y = (\sigma/\sigma_y)^{1/N} \quad \text{for } \varepsilon \geqslant \varepsilon_1, \end{aligned} \tag{2a}$$

or

$$\sigma = \sigma_y + K(\varepsilon - \varepsilon_y)^{N_1} \quad \text{for } \varepsilon \geqslant \varepsilon_y. \tag{2b}$$

Here, $\varepsilon_y = 0.0035$ the yield strain, $\varepsilon_1 = 0$–0.03 is the Luder's-type strain and $N = 0$–0.2. For Eq. (2b), $N_1 = 0.3$ and $K = 400$ MPa. Since various σ-models were used the $R = \sigma^*/\sigma_y$ was generally specified in terms of a fraction of the peak stress ($\sigma_{22\max}$) for a particular constitutive law, as $R = h\sigma_{22\max}/\sigma_y$, where $h = 0.75$, 0.85 and 0.95.

Using the relation $K = \sqrt{EJ}$ the FE toughness adjustment results can be expressed as

$$J/J_{ssy} = f(R, M^{-1}). \tag{3a}$$

Here

$$f(R, M^{-1}) = \sum_{i=1-4} \lambda_i(M^{-1}) R_i, \tag{3b}$$

where the λ_i are related to M though a set of coefficients (c_{ij}) fit to the FE results as:

$$\lambda_i = \sum_{j=1-3} c_{ij} M^{-j}. \tag{3c}$$

We assume a MC shape given by [8]

$$K_{mc}(T) = 30 + 70\exp[0.019(T - T_{or})] \quad (\mathrm{MPa}\sqrt{\mathrm{m}}), \quad (4)$$

where the T_{100} is the T_{or} for $K_{Jcr} = 100$ MPa$\sqrt{\mathrm{m}}$. Thus

$$K_{Jcr} = K_{mc}(T_{ocl})[f(R, M^{-1})]^{1/2}, \\ = K_{mc}(T_{ocl})\{f[R(T_{or}), K_{Jcr}^2/Eb\sigma_y(T_{ocl})]\}^{1/2}. \quad (5)$$

We use an empirical fit to $\sigma_y(T)$

$$\sigma_y(T) = 515.2 + 0.9327T + 0.002069T^2 \\ - 1.288 \times 10^{-5}T^3 + 8.622 \times 10^{-8}T^4 \\ - 1.512 \times 10^{-10}T^5, \quad (6)$$

where T is in °C. Specifying T_{or}, K_{Jcr}, R and the constitutive law Eqs. (4)–(6) can be solved for T_{ocl}, hence ΔT_{cl}, as a function of M or for a given σ_y and b.

3. Results and discussion

Fig. 1 shows T_{ocl} as functions of $1/b$ for $N = 0.1$, $T_{or} = -20$ °C, $h = 0.75$, 0.85 and 0.95 ($R = \sigma^*/\sigma_y = 2.72$, 3.09 and 3.44) and $K_{Jcr} = 100$ MPa$\sqrt{\mathrm{m}}$. The results show that as expected T_{ocl} decreases with decreasing b and R. Fig. 2 shows the effects of varying T_{or} from −60 to 20 °C on ΔT_{cl} for $N = 0.1$, $R = 3.09$ and $K_{Jcr} = 100$ MPa$\sqrt{\mathrm{m}}$. The ΔT_{cl} increases with increasing T_{or}. Fig. 3 shows T_{ocl} as a function of $1/b$ for various constitutive equations for $R = 2.774$, and 2.482 (lower R are needed to ensure that $\sigma^* < \sigma_{22\,max}$ for all the cases), $T_{or} = -60$ °C and $K_{Jcr} = 100$ MPa$\sqrt{\mathrm{m}}$. The ΔT_{cl} increases with lower stain hardening and higher levels Luder's-type strain. The effects of K_{Jcr} on the T_{ocl} are shown in Fig. 4 for $T_{or} = -60$ °C and $K_{Jcr} = 60$, 80 and 100 MPa$\sqrt{\mathrm{m}}$ and $R = 2.72$ and 3.44. The T_{ocl} increases with higher K_{Jcr} and lower R.

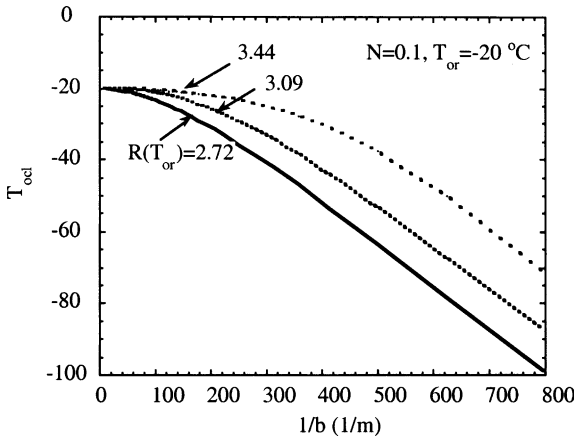

Fig. 1. T_0 as a function of $1/b$ for $R = 2.72$, 3.09 and 3.44, $N = 0.1$, $T_{or} = -20$ °C and $K_{Jcr} = 100$ MPa$\sqrt{\mathrm{m}}$.

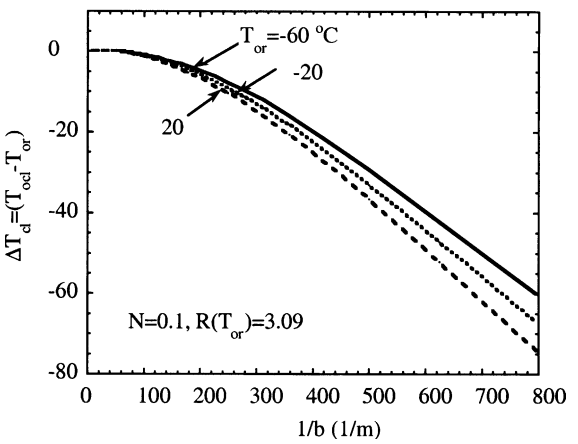

Fig. 2. The effects of T_{or} on ΔT_{cl} is for $N = 0.1$, $R = 3.09$ and $K_{Jcr} = 100$ MPa$\sqrt{\mathrm{m}}$.

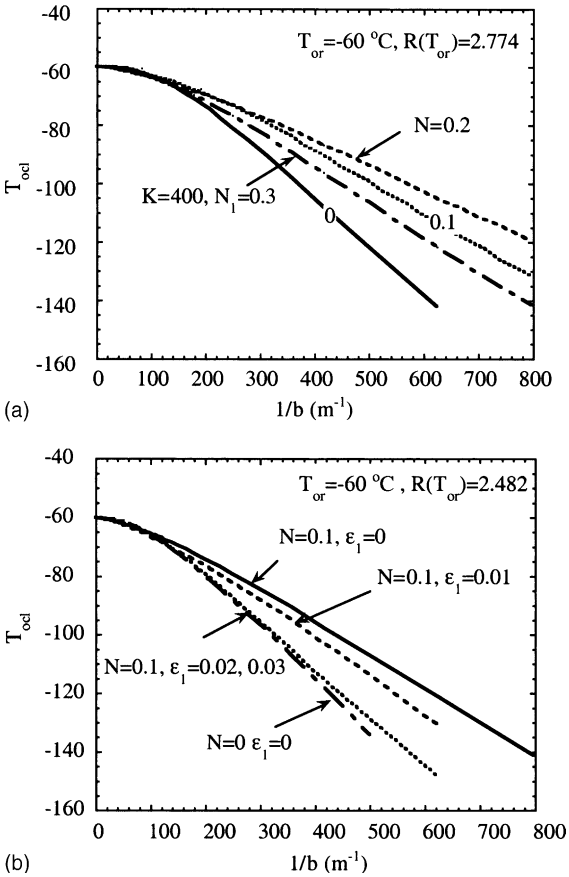

Fig. 3. T_0 as a function of $1/b$ for various constitutive equations for $T_{or} = -60$ °C and $K_{Jcr} = 100$ MPa$\sqrt{\mathrm{m}}$, (a) $R = 2.774$, (b) $R = 2.482$.

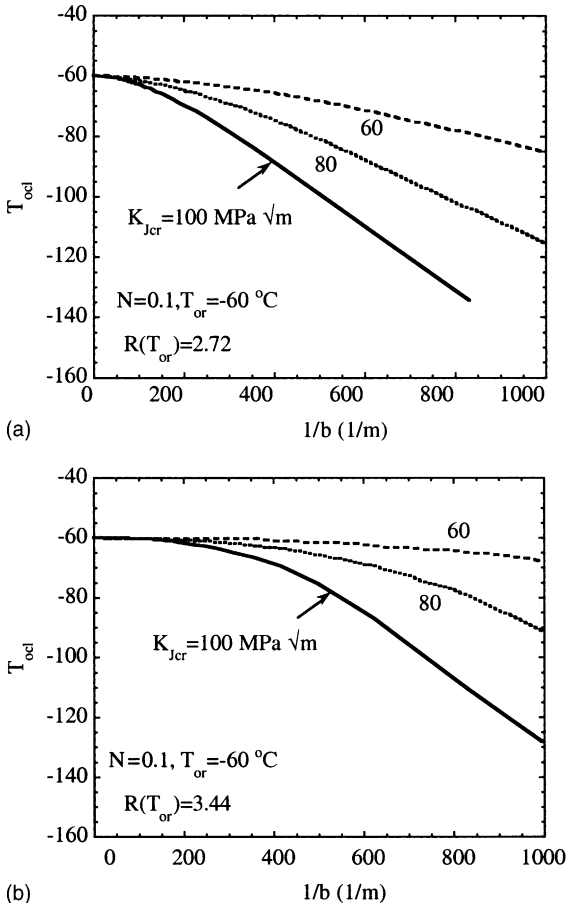

Fig. 4. The effects of K_{Jcr} on the ΔT_{cl} for $K_{Jcr} = 60$, 80, and 100 MPa$\sqrt{m}$ (a) and for $R = 2.72$, and (b) $R = 3.44$.

These results indicate that for most expected cases involving relatively high R, low T_0 and moderate strain hardening, the ΔT_{cl} should be moderate ($\lesssim$40 °C) down to b as small as about 0.2 mm or less, even for the nominal $K_{Jcr} = 100$ MPa$\sqrt{m}$. The ΔT_{cl} increases at lower strain hardening characteristic of irradiated alloys. However, by using a somewhat lower K_{Jcr} of $\approx$60–80 MPa$\sqrt{m}$ the ΔT_{cl} should be moderate even for low strain hardening materials.

The results of 3D finite element calculations [4] show somewhat larger J/J_{ssy} than the 2D plane strain estimates in this work for $M < 100$. However, the general trends are similar. Statistical effects also result in a lower T_0 in smaller specimens because of the reduced high stress volume [4]. This statistical effect can also be expressed in terms of a corresponding ΔT_{os}, which is about -30 °C for $b = 2$ mm compared to, for example, a specified reference value of 10 mm. However, higher loading rates result in upward shifts of the T_0, hence, can compensate for both the CL and statistical shifts at smaller sizes. These loading rate shifts depend on T_{or}, but are typically of order 50–60 °C. This has led to the development of a impact tested 1/6-size PCC specimen that gives a net T_0 in the range of that for a static at a dynamic K_{Jcr} of about 70 MPa$\sqrt{m}$ [9].

These results should be viewed as a step towards a more complete treatment of size effects of transition toughness. For example, Rathbun et al. have recently carried out an extensive experimental-analytical study of size effects in a pressure vessel steel to develop a full 3D models of the combined effects of CL and statistical stressed volume effects [3,10], including the effects of out of plane CL. When corrected for both effects, data for an enormous range of specimen sizes fall in the same toughness population. The calibrated 3D models also worked fairly well on shallow crack and very small specimens, albeit not perfectly. Indeed, the pressure vessel steel results are broadly consistent with even more recent dynamic tests on the ultra-small 1/6-size PCC specimens cited above [9] that show somewhat lower toughness than would be predicted by the 3D models. The pressure vessel steel data also indicate a relative insensitivity of *minimum* toughness values to size effects. Thus additional research is needed to clarify the limitations and to refine the physical basis for existing size effects models.

4. Summary and conclusions

A systematic assessment of the effects of material constitutive and local fracture properties on CL in fracture toughness tests of small specimens was carried out within the framework of the MC-ΔT method. In this context CL results in a downward shift in the temperature ΔT_{cl} at a specified reference toughness, K_{Jcr}. The results show that ΔT_{cl} increases with decreasing: (a) specimen size, (b) the ratio of the critical cleavage stress to yield stress at the reference toughness and (c) the strain-hardening rate. The ΔT_{cl} increases with higher K_{Jcr} and the reference toughness–temperature, T_{or}. These results support the use of small fracture specimens for referencing $K_{Jc}(T)$ curves for cases when the ΔT_{cl} are modest, assuming the shifts are properly evaluated. Even smaller specimens with larger ΔT_{cl} may still be useful, since the basic mechanisms and mechanics of cleavage remain similar to that experienced in larger test-pieces. However, since the ΔT_{cl} increase with the reference toughness in this case, the corresponding $K_q(T)$ curves are extremely steep in the transition. This can be an advantage for purposes of comparing the effects of a particular variable on the ΔT_{irr} [9]. Additional statistical effects of size as well as loading rate were also noted. While both CL and statistical effects result in downward shifts in T_0, higher loading rates have the opposite, partially compensating effect.

References

[1] G.R. Odette, K. Edsinger, G.E. Lucas, E. Donahue, Small Specimen Test Techniques, ASTM STP 1329, 1998, p. 298.
[2] R.O. Ritchie, J.F. Knott, J.R. Rice, J. Mech. Phys. Solids 21 (1973) 395.
[3] H.J. Rathbun, G.R. Odette, M.Y. He, in: K. Ravi Chandar et al. (Eds.), Advances in Fracture Research, Proceedings of Tenth International Congress on Fracture, 2001, in press.
[4] G.R. Odette, M.Y. He, J. Nucl. Mater. 283–287 (2000) 120.
[5] T.L. Anderson, D. Steinstra, R.H. Dodds, Fracture Mechanics, 24, ASTM STP 1207, 1994, p. 186.
[6] M. Nevalainen, R.H. Dodds, Int. J. Fract. 74 (1995) 131.
[7] ABAQUS Version 5.8, Hibbitt Karlsson and Sorenson, Providence, Rhode Island, 1998.
[8] ASTM E 1921–97, 2001 Annual Book of ASTM Standards V03.01, 2001.
[9] G.R. Odette, M. He, D. Gragg, D. Klingensmith, G.E. Lucas, these Proceedings.
[10] H.J. Rathbun, G.R. Odette, M.Y. He, G.E. Lucas, T. Yamamoto, Size Scaling of Cleavage Toughness in the Transition: A Single Variable Experiment and Model-Based Analysis, NUREG/CR-6790, 2003 (in press).